

Path-Constrained Rendezvous: Necessary and Sufficient Conditions

K.M. Soileau*

NASA Johnson Space Center, Houston, Texas

and

S.A. Stern†

University of Colorado, Boulder, Colorado

The problem of path-constrained rendezvous in the vicinity of a Large Space Structure (LSS) was first introduced some years ago. Our contribution to this field centers on a demonstration that the problem can be reduced from a path-constraint problem to one of end-point constraints or certain (common) Large Space Structure geometries, under the assumption of an unrestrictive upper limit on the transfer time. This finding has been made under the assumption of a circular Keplerian orbit, and has been normalized with respect to orbital semi-major axis and LSS size. In addition to demonstrating this important simplification of the of the path-constrained rendezvous problem, we also discuss the results of numerical simulations of path constrained transfers from point-to-point on large spherical structures in orbit, and derive a series of conclusions having both architectural (design) and operational implications for LSS designers/operators.

Nomenclature

CW	= Clohessy-Wiltshire
FZ	= forbidden zone
GEO	= geosynchronous Earth orbit
H	= cylindrical LSS height
LEO	= low Earth orbit
LSS	= Large Space Structure
MTV	= Maneuvering Transfer Vehicle
\hat{n}	= LSS local surface normal unit vector
r	= LSS radius
R	= the distance metric function
t	= time, s
TC	= tangential conditions
TAC	= tangential arrival condition
TDC	= tangential departure condition
V	= velocity
\hat{x}	= CW unit vector antiparallel to the orbital velocity
\hat{y}	= CW unit vector parallel to the orbital radius vector
\hat{z}	= CW unit vector parallel to the orbital angular momentum vector
x_c, y_c, z_c	= FZ center to Target Point Vector x , y , and z coordinates, respectively
τ	= transfer time, s
θ	= transfer angle, deg
θ_{\min}	= minimum path-avoiding transfer angle
θ_{crit}	= greatest transfer angle for which the TC's are sufficient conditions
ω	= orbital angular rate

I. Introduction

THE problem of path-constrained rendezvous was first introduced by Stern.¹ A simple statement of the general problem of path-constrained rendezvous can be made as follows: How it is possible to maneuver from point to point about an orbiting Large Space Structure of arbitrary size,

geometrical configuration, and spin, to avoid those transfer paths which pass through the structure itself? Classical rendezvous guidance equations leave the path between the departure and arrival points unconstrained. In this problem, it is necessary to determine how a transfer can be constructed to achieve target intercept *and* avoid the constraint imposed by the presence of the LSS itself.

Path-constrained rendezvous in the vicinity of Large Space Structures has relevance to many operational scenarios for space development and exploration, including LSS construction, LSS maintenance, space station operations, solar power satellite planning, and asteroid mining, to name a few. It has been demonstrated² that path-constrained rendezvous will be an important factor for structures as small as the currently planned U.S. Space Station.

Stern and Fowler³ have recently published an empirical study of the problem of operational path-constrained rendezvous. Through the use of extensive numerical simulations, it was shown that, in general, only a small fraction of the possible unbroken (i.e., no corner condition) paths connecting arbitrary points on LSS's—represented by sphere-like, plate-like, and straw-like LSS geometries—successfully complete arbitrary point-to-point transfer without first colliding with the imposed path constraint. Many unsuccessful (penetrating) transfer paths were found to fail at the departure point, as the guidance equations attempted to drive through the constraint surface approximately along the line of sight to the target. It was also shown that transfer success difficulty was proportional to the proximity of the departure and arrival points to the constraint surface, so that the most difficult transfers to successfully accomplish were those between two point on the LSS. These authors also demonstrated the dependance of a prior success likelihood on the LSS's geometry and attitude.

As a final contribution, these authors showed that although success was unlikely for a classical single (i.e., transfer injection) impulse transfer, a broken-path, two-impulse transfer resulted in success probability approaching unity. Such two-impulse transfers involve finding a suitably chosen "way-point" for an initial target, at which a second maneuver, redirecting the path toward the intended final destination, can be made. Stern and Fowler found that a good location for the waypoint target was approximately halfway between the departure and destination points, but placed directly above the constraint surface at an "altitude" approximately equal to the minimum distance from which both the departure and arrival points could be simultaneously viewed.

Received April 29, 1985; revision received Oct. 20, 1985. Copyright © 1986 by S.A. Stern. Published by the American Institute of Aeronautics and Astronautics, Inc., with permission.

*Aerospace Technologist.

†Research Associate, Laboratory for Atmospheric and Space Physics. Member AIAA.

In this paper, we define formally the general problem of path-constrained rendezvous in the vicinity of large constraint surfaces. We then proceed to state a pair of conditions necessary for the completion of a successful (i.e., non-impacting) transfer between points on the LSS, and show that these conditions turn out to be sufficient (subject to a transfer time constraint) for the successful completion of such transfers, at least for the useful LSS geometries which we tested. Finally, we employ these conditions in a case study of a nondimensionalized spherical LSS, from which we discover a number of "rules" that enable us to make general statements about preferred architectural configurations and operational rendezvous techniques.

II. Background

To study transfer paths connecting two arbitrary points on the surface of a Large Space Structure, we first define the constraint surface itself. For theoretical reasons, we introduce the useful concept of a Forbidden Zone (FZ), defined here as any large unpassable volume in orbit which can be represented by a constraint surface. The FZ can be open or closed, and may be of positive or negative curvature; indeed the only requirement placed upon FZ geometry is that it be a connected region.

Defined in this way, an FZ could either be a physical volume (e.g., an LSS, a space station, or an asteroid), or a non-physical volume (e.g., an antenna radiation avoidance zone). It could have holes in its walls (e.g., tunnels), and could be open at one end (e.g., a large antenna).

The goal of path-constrained rendezvous research is to describe how a maneuvering vehicle in close proximity to an FZ can maneuver between arbitrary points exterior to the FZ constraint surface without contacting (i.e., colliding with) the FZ, except at the endpoints of the transfer path. Preferably, any scheme for finding noncolliding paths should be operationally useful, and should therefore avoid undue complications. Classically, the maneuvering vehicle is assumed to be of much smaller dimensions than the FZ itself, so that the transfer problem is reduced to a point mass operating in the vicinity of a constraint surface; an example of such a case would be an astronaut maneuvering from one side of a Large Space Structure to another. In this paper, we also assume that the mutual gravitational attraction of the FZ and the Maneuvering Transfer Vehicle (MTV) is insignificant, so that the transfer retains its identity as a classical Keplerian relative motion problem, save for the path constraint imposed by the FZ itself. These restrictions are primarily introduced as a part of the formalism, and do not restrict the practical applicability of our results. Specific applications which are excluded by these simplifying assumptions are operations in the vicinity of an asteroid (where the perturbing mass is significant), and the terminal rendezvous and proximity operations of a Space Shuttle near the envisioned space station (which is of similar dimensions to the Shuttle).

Various authors⁴⁻⁶ have discussed the merits of a set of rendezvous targeting equations which were first derived by Hill in 1878, and later rediscovered by Clohessy and Wilshire in 1960. These time-parametric equations are achieved by linearizing the differential equations of relative motion for a massless point in circular orbit about the center of mass of a spherical body. The solution to these equations is commonly known as the CW Equations of relative motion and has been widely used for operational rendezvous guidance aboard Gemini, Apollo, and Shuttle spacecraft.

Chief among the merits of the CW equations are their ease of application and their great accuracy for transfer times as long as one-quarter of the orbital period.⁷⁻⁹ Such transfer times make possible accurate traverses of several kms on low Earth orbit (LEO) and many kms in Geosynchronous Earth orbit (GEO). Because these path lengths exceed the likely dimensions of any LSS/FZ planned or envisioned for the foreseeable future, it is possible to use the CS equations in the

analysis of transfer between points on LSS's. Should LSS's eventually exceed even these dimensions, further improvements to the rendezvous guidance equations (such as those employed by London¹⁰ may be necessary.

Without development, we present here the CW relative motion equations:

$$x(t) = 2 \left(\frac{\dot{x}_0}{\omega} - 3y_0 \right) \sin(\omega t) - 2 \frac{\dot{y}_0}{\omega} \cos(\omega t) \quad (1a)$$

$$+ \left(6y_0 - 3 \frac{\dot{x}_0}{\omega} \right) \omega t + 2 \frac{\dot{y}_0}{\omega} + x_0$$

$$y(t) = \left(2 \frac{\dot{x}_0}{\omega} - 3y_0 \right) \cos(\omega t) + \frac{\dot{y}_0}{\omega} \sin(\omega t) - 2 \frac{\dot{x}_0}{\omega} + 4y_0 \quad (1b)$$

$$z(t) = z_0 \cos(\omega t) + \frac{\dot{z}_0}{\omega} \sin(\omega t) \quad (1c)$$

where ω is orbital angular rate, and t is elapsed time. The rotating Cartesian coordinate system employed (Fig. 1) exhibits \hat{x} in the orbital plane antiparallel to the velocity vector, \hat{y} directed radially outward from the Earth's center through the coordinate origin, and \hat{z} completing the right-handed triad.

Equation (1) can be used to target a rendezvous intercept by locating the coordinate system origin at the desired transfer end-point and then forcing the x , y , and z separations to zero (i.e., rendezvous) after some time τ , which we refer to as the transfer time. Solving in this way the initial velocities \dot{x}_0 , \dot{y}_0 , and \dot{z}_0 required to effect intercept are

$$x_0(\tau) = \frac{x_0 \omega \sin \phi + y_0 \omega [6 \phi \sin \phi - 14(1 - \cos \phi)]}{3 \phi \sin \phi - 8[1 - \cos \phi]} \quad (2a)$$

$$y_0(\tau) = \frac{2 \omega x_0 [1 - \cos(\phi)] + y_0 \omega [4 \sin \phi - 3 \phi \cos \phi]}{3 \phi \sin \phi - 8[1 - \cos \phi]} \quad (2b)$$

$$z_0(\tau) = \frac{-\omega z_0}{\tan(\theta)} \quad (2c)$$

It is worth noting that although it is necessary to null all velocities at target intercept in order to effect a rendezvous, we will not be concerned with such a maneuver here. This is because it is not necessary to restrict transfer behavior at or

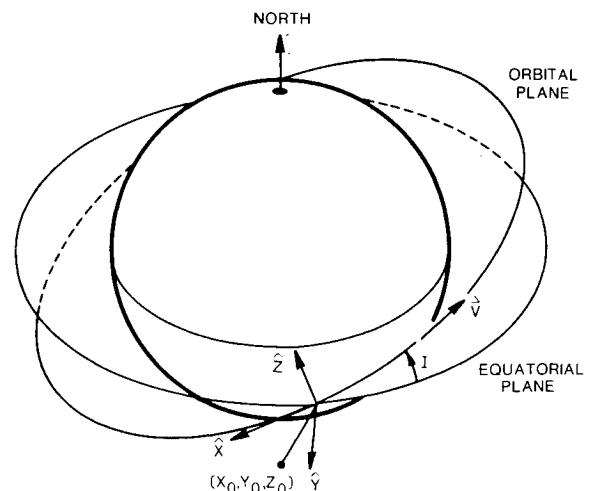


Fig. 1 The CW coordinate system and its relationship to the orbit; the coordinate system rotates about the Earth at orbital angular rate ω .

after the successful intercept itself. We note, however, that the magnitude of the stopping maneuver is of interest to the eventual cost-optimization of the path-constrained rendezvous problem.

III. Problem Statement

We are now in a position to describe analytically success criteria for the path-constrained rendezvous problem. Simply put, we require the distance metric R from the Maneuvering Transfer Vehicle to the nearest point on the FZ surface to remain positive throughout the transfer:

$$R(t) > 0 \quad \text{for} \quad t \in (0, \tau) \quad (3)$$

This generalized criteria will ensure clearance throughout the transfer by forcing the transfer path to lie entirely exterior to the FZ, except at the end points.

The metric $R(t)$ is a function of the shape, size, and rotational history of the FZ under consideration. As in past work, it is useful to restrict the FZ geometry to a few well-known shapes which closely match the larger elements of any likely forbidden zone. These primary FZ's include the sphere, the hemisphere, the straw (a cylinder with height \gg radius), the plate (a cylinder with radius \gg height), and the cone. Each of these primary FZ's contain important mathematical symmetries which make them tractable for study. We point out that real space structures with bristling antennae, hatches, thrusters, and other "microdetails" can be encapsulated in a primary FZ with the same shape as, and only slightly larger than, an FZ which represents the gross structure itself; the use of such non-optimal forbidden zones does not effect the results obtained in this research. Highly complex structures can be represented by a Tinkertoy agglomeration of simple forbidden zones.

Figure 2 depicts a representative successful transfer about a sphere. We assume that the FZ is corotating in lock-step with the CW coordinate system, so that the departure and target points are fixed in the CW frame and the constraint surface is scleronomic.

For spherical Forbidden Zones, the success criteria may be written:

$$[x(t) - x']^2 + [y(t) - y']^2 + [z(t) - z']^2 - r^2 > 0 \quad \text{for} \quad t \in (0, \tau) \quad (4)$$

where r is the radius of the sphere, x' , y' , and z' describe the time-invariant components of the transfer FZ-center to target point vector, and $x(t)$, $y(t)$, and $z(t)$ are the time-varying

coordinates of the target vehicle as it traverses from its departure to its target point. $x(t)$, $y(t)$, and $z(t)$ are given by Eq. (1) after the solution for \dot{x}_0 , \dot{y}_0 and \dot{z} in Eq. (2). When these substitutions are made, Eq. (4) becomes quite complex:

$$\begin{aligned} & \left(\frac{3B^2}{8} + \frac{z_0^2}{2} - \frac{F^2}{2} \right) \cos 2\theta + (z_0 F) \sin 2\theta \\ & + (2BD + 2AE - 2y_c A - 2x_c B - 2z_c z_0) \cos \theta \\ & + (2AD + BE - 2x_c A + By_c - 2z_c F) \sin \theta \\ & + (2AC)\theta \sin \theta + (2BC)\theta \cos \theta + C^2 \theta + (2CD - 2Cx_c)\theta \\ & + \left(-2z_c D - 2y_c E + [x_c^2 + y_c^2 + z_c^2] + A^2 + \frac{5B^2}{8} \right. \\ & \left. + D^2 E^2 + \frac{F^2}{2} + \frac{z_0^2}{2} \right) - r^2 \geq 0 \end{aligned} \quad (5)$$

where the coefficients A , B , C , D , E , and F , which are derived from the coefficient terms in Eq. (1), are

$$\begin{aligned} A &= 2 \left(\frac{\dot{x}_0}{\omega} - z y_0 \right) & D &= \frac{2y_0}{\omega} + x_0 \\ B &= 2\dot{y}_0/\omega & E &= \frac{-z\dot{x}_0}{\omega} + 4y_0 \\ C &= 6y_0 - \frac{z\dot{x}_0}{\omega} & F &= \dot{z}_0/\omega \end{aligned}$$

and where \dot{x}_0 , \dot{y}_0 , and \dot{z}_0 are given by Eq. (2).

Similarly to Eq. (4), the success criteria for transfers about the side-walls of straw-like FZ can be written as:

$$[x(t) - x']^2 + [y(t) - y']^2 + r^2 > 0 \quad \text{for} \quad t \in (0, \tau) \quad (6)$$

whenever the criteria $|z(t) - z'| < H/2$ simultaneously obtains, and where H is the height of the cylinder.

The expansion of Eq. (6) has an even more cumbersome result than does Eq. (5), as do the expansions resulting from the metrics relating to hemispheres, plates, and cones.

Attempts at obtaining a general root-finding solution to the nine-variable ($x_0, y_0, z_0, x_c, y_c, z_c, \omega, r, \tau$) success criteria, which would instruct us how to maneuver between arbitrary points on the FZ surface, rapidly grow to practical intractability due to the multiplicity of algebraic terms resulting from the full differentiation of the distance metric [e.g., Eq. (5)]. Stern and Fowler solved this dilemma by making numerical simulations of the problem and searching for statistical guides to success likelihood. Here, we attack the problem from a different perspective, by finding necessary and then sufficient conditions for success likelihood.

IV. Necessary Conditions

We now want to place the results obtained by Stern and Fowler on firmer theoretical footing. In particular, we want to know if successful transfers in the vicinity of a forbidden zone can be found from analytical conditions relating only to the end-point (departure and arrival conditions) and the FZ geometry. Such a solution would effectively reduce the path constraint problem outlined above to a two-point boundary value problem similar in form to classical relative-motion rendezvous mechanics.

Successful transfers from any point on an FZ surface to another such point must satisfy at least two point-conditions: 1) they must depart along a path away from the FZ, and 2) intercept the target from above the FZ surface.

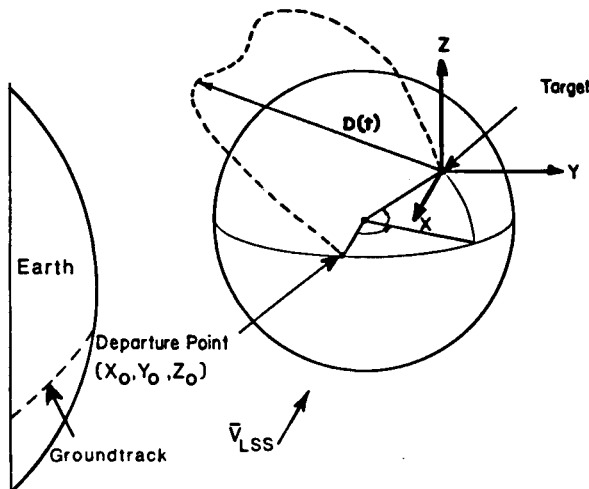


Fig. 2 A representative successful transfer about a spherical forbidden zone. Notice the FZ "equator" lies in the orbital plane.

We call the first of these conditions the tangential departure condition (TDC), since it forces the Maneuvering Transfer Vehicle to depart at least tangentially from the FZ surface. For analogous reasons, we call the second condition the tangential arrival condition (TAC). In effect, these two conditions, which hold for any FZ geometry (even rotating FZ's), require the transfer to at least begin and end in a manner consistent with success.

Analytically, the tangential departure/arrival conditions may be stated as inequality constraints on the dot product of the departure/arrival velocity vectors and the local FZ surface normal:

$$\hat{n} \cdot V_0 > 0 \quad (\text{TDC}) \quad (7a)$$

$$\hat{n} \cdot V_f < 0 \quad (\text{TAC}) \quad (7b)$$

We call attention to the fact that denominators $|\hat{n}| |\hat{V}|$ in Eq. (7) has been removed because this multiplicative factor in the dot product formulation is positive, and will not effect the results of the inequality checks required by these equations. As a corollary to Eq. (7), it can be seen that the number of extrema in R , for any successful transfer, must be at least one (since we must turn around between departure and arrival); if greater than one, the number of extremas must be odd-numbered.

From the twin necessary conditions represented by Eq. (7), it is possible to restrain surface by CW paths. Although we will use such a technique later as part of a case study, we first devote attention to the description of an important discovery: the tangential conditions provide both *necessary and sufficient* condition for successful transfers about spheres, plates, and straws, under the assumption of a transfer time limit.

V. The Tangential Conditions: A Sufficiency Demonstration

To study the behavior of those cases which were successful and also satisfied the tangential departure and arrival conditions, we constructed a numerical computer simulation. In this simulation, flight trajectories were defined by nested do-loops which varied the parameters $x_0, y_0, z_0, x_c, y_c, z_c$ (thus x_f, y_f, z_f). For each such case, the program first evaluated the tangential conditions; if both the TDC and the TAC were successfully satisfied, the program then computed a history of the behavior of the success criteria described above. This function was evaluated at 300 evenly spaced points along the path.

We investigated spherical as well as both plate-like and straw-like forbidden zones. Table 1 summarizes the cases run in our analysis. In the cases of plate-like FZ's the cylindrical constraint surface was defined with a radius to height of 3:1; similarly, for the straw-like FZ's in our study, the radius to height was set at 1:3. Cases were run for each of these two FZ's, with the axis of symmetry directed along \hat{x} , \hat{y} , and \hat{z} CW coordinates. In this way, we were able to explore the effect of the variation in FZ attitude to the CW coordinate frame. We note that these orthogonal attitudes contain within them the gravity gradient and local horizontal, as well as the minimum drag cases.

We found it possible to normalize the constraint equations, as well as both the tangential conditions themselves by β , the

orbital angular rate, as well as by the major dimension of the FZ; in this way we were able to remove two variables, ω and r , from our sample space. As a result of this normalization, the results presented here are independent of orbit altitude and FS size and therefore represent an important generalization over past work in this field.

The sample space which we tested included 6561 combinations of uniformly distributed in-plane, on-the-FZ "longitude," and each of which were tested for nine equally spaced transfer angles θ (i.e., transfer time/orbit period) ranging from 5 to 89 deg. The use of uniformly distributed cases allows us to compute correlation statistics according to the well-known $1/\sqrt{n}$ theorem for counting statistics. This data set produces a confidence level of 0.9959 in our results.

Our choice of the range of θ was limited to transfers of less than 90 deg because the CW equations lose accuracy after this point; we note that quarter-orbit transfer (24 min at LEO, 6 h at GEO) are operationally suitable, and do not impose undue restrictions on average transfer velocity.

From the data in Table 1 we find that for the sphere, as well as both straws and plates in each of three operationally important attitudes, the tangential department and arrival conditions strongly correlate with transfer success (non-collision along the path) for transfers over the span of transfer angle ($\theta < 90$ deg) allowable by the CW equations. Further analysis proved that the correspondence between the TC's and success held in *all* cases for $\theta < \theta_{\text{crit}}$, where θ_{crit} was found to be a function of FZ geometry and attitude. We therefore conclude that the sufficiency of the twin TC's is valid up to an unrestrictive transfer angle (time) constraint on θ . The significance of θ_{crit} , the upper limit on the transfer angle, will be discussed later.

While we still find (in agreement with Stern and Fowler's earlier work) that a priori success probability for a transfer between arbitrary points on these primary forbidden zones is unlikely (i.e., ranging approximately between 15 and 40%), we have made the *important* discovery that success can be predicted by examining the endpoint trajectory conditions alone (at least up to an unrestrictive transfer time constraint). Refer to Stern and Fowler's work for a detailed discussion of success likelihood as a function of FZ geometry and attitude.

This finding makes feasible a much greater variety of numerical simulations than had been previously possible, by reducing the necessary computational load inherent in each test case. More important, this finding makes the task of finding a successful transfer in the operational environment tremendously easier. This is because it is no longer necessary to numerically "fly" each possible trajectory between the departure and destination. Instead, one need only check the endpoints of the transfer for the inequality tests given in Eq. (7); should these conditions hold, trajectory will be path avoiding (so long as θ [τ] exceed θ_{crit} [τ_{crit}]). We add that, because the TC's are necessary conditions, one is assured that should these conditions fail, the trajectory is sure to fail. We note that although the nature of our numerical sufficiency demonstration cannot guarantee a safe (noncolliding) trajectory based only upon these tests, the probability of successful making a transfer which passes Eq. (7) when the θ_{crit} constraint is applied is so high (at least 0.9959, our statistical confidence level) that at most one might numerically "fly" the chosen path to check for FZ clearance, expecting less than one

Table 1 Correlation between TAC, TDC and success

Case	Cases run	Fraction satisfying TC's	Fraction of successful cases satisfying TC's	θ_{crit} , deg
Sphere	59,049	0.0489	0.9948	57
Plate x	59,049	0.2307	0.9988	58
Plate y	59,049	0.2115	0.9987	58
Plate z	59,049	0.3980	0.9999	55
Straw x	59,049	0.1087	0.9824	40
Straw y	59,049	0.1290	0.9688	40
Straw z	59,049	0.1745	0.9979	55

failure in 200 trajectories that pass these tests. Future tests with an even larger sample space could raise the confidence factor in the sufficiency demonstration to an even higher level. In Sec. VI we apply this result to a case study of the behavior of those regions on spherical forbidden zones which can be successfully connected by a single-burn transfer path entirely exterior to the FZ surface.

Before examining this important test case, we first discuss the nature and the behavior of the constraint $\theta < \theta_{crit}$ for sufficiency. We found through our simulations that all cases in which the TC's were passed, but where there was FZ penetration along the route to the target point, occurred above some critical value of θ , the transfer angle. This means that the TC's always satisfied the sufficiency test whenever θ was less than θ_{crit} . Why is this so? A brief motivating discussion follows.

It is clear from earlier studies² that as the transfer angle θ is shortened, the path described by the CW equations during a directed rendezvous becomes increasingly rectilinear. Therefore, where θ is sufficiently short, the CW equations will, regardless of the starting and stopping points (and independent of the FZ geometry, of which they are not "aware"), force the necessary conditions in Eq. (7) to fail by attempting to cut directly through the FZ on their way to the destination target. Conversely, as the value of θ increases, the CW rendezvous trajectory becomes increasingly curvilinear. It is our finding that up to some limiting time, the TC's contain sufficient information about the path curvature at the endpoints to ensure that the path curvature between the departure and destination is both exterior to the FZ and that the metric R is without zeros (crashes). This is not doubt due to the topology of the CW paths.

We conclude this section with a discussion of the θ_{crit} data presented in Table 1. θ_{crit} , one recalls, is the greatest value of the transfer angle for which the sufficiency of the tangential conditions holds. The data presented in Table 1 are the result of an expanded run in which the density of $(x_0, y_0, z_0, x_c, y_c, z_c)$ was increased by a factor of 10, and θ_{crit} was determined to one-deg accuracy. It can be seen upon examination of this data that: a) θ_{crit} is a function of LSS geometry (shape, plate, or cylinder); b) θ_{crit} is a function of LSS attitude; and c) θ_{crit} is operationally unrestricted. Conclusion (c) is most important, for it implies that the sufficiency of the TC's applies over a suitably wide range of transfer angles (or times), such that this sufficiency may be considered operationally useful.

VI. A Case Study

As reported in the Introduction, previous studies have established the difficulty of making transfers between arbitrary points on a forbidden zone surface when the transfer guidance scheme is restricted to the single-impulse scheme typically used for terminal-area maneuvering, and the path between points is unconstrained. With the tangential conditions in hand, it now becomes feasible to compute many more simulated trajectories than was previously possible, and to use the results of such large-scale simulations to discern important trends in the behavior of the success criteria as a function of departure location, arrival location, and transfer time.

Before presenting our test case, we first ask whether it is possible to make broad conclusions about those points which cannot be connected by a noncolliding CW path. The TC constraint equations contain sufficient information to answer such a question in the affirmative. One example of a class of points which cannot be connected by a non-colliding CW transfer are the class of "purely out-of-plane" transfers. In this context, "purely out-of-plane" refers to a transfer from any point on the spherical FZ to another point separated only in the out-of-plane coordinate z , which corresponds to points separated only by a "latitude" reflection through the equator of the sphere. Such destination points lie on the sphere at the same "longitude" but the "opposite latitude" of the departure point. Because the CW equations decouple z (out-of-plane) motion from x, y (in-plane) motion, it can be seen that

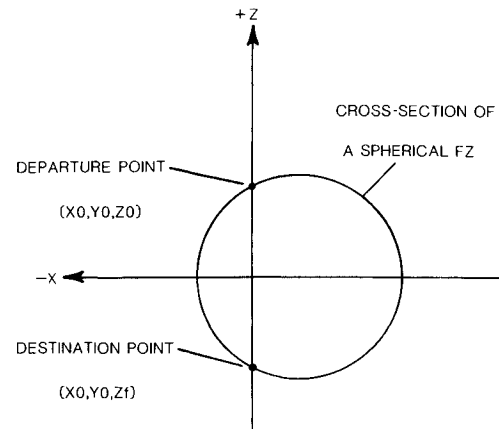


Fig. 3 A schematic cross-section of a spherical FZ illustrating the impossibility of purely out-of-plane transfer for such forbidden zones.

the CW equations can only cause a "vertical" transfer to occur when no x and y separation exist. Therefore, purely out-of-plane transfers must pierce the FZ as it cuts across the chordline connecting the departure and destination points. By examining Fig. 3, in which such a transfer is depicted, it can be seen that both TAC and the TDC constraints must always be violated in any such transfer; evaluating Eq. (7) also shows this type of transfer to be identically unsuccessful. We conclude from this example that: a) the TDC and TAC can provide us with general information leading to the general inclusion and exclusion of various classes of transfers; and b) some general classes of transfers can be conclusively shown to be impossible in the context of spherical FZ's.

Further examination of the TC's leads us to find that the FZ geometry and attitude relative to the orbital coordinate frame is an important factor in the question of accessibility. This is amply demonstrated by the fact that the very same out-of-plane transfers that have been demonstrated to be impossible for spherical FZ's are always possible for strawlike FZ's oriented with the long axis of the cylindrical FZ parallel to the \hat{z} direction, so that no protruding surface ever exists between points on the straw separated only by latitude. In this case, the CW z decoupling allows us to "skate" up and down the cylindrical sidewall without collision. Other conclusions along these lines are too numerous to warrant inclusion here; we instead defer to the powerful and general nature of the tangential conditions. We now turn to the results obtained from the spherical FZ case study.

For a spherical FZ, the tangential conditions can be written as:

$$\dot{x}_0(x_0 - x_c) + \dot{y}_0(x_0 - y_c) + \dot{z}_0(x_0 - z_c) > 0 \quad (8a)$$

$$\dot{x}_f(0 - x_c) + \dot{y}_f(0 - y_c) + \dot{z}_f(0 - z_c) < 0 \quad (8b)$$

where the subscript f refers to the final velocities as the Transfer Vehicle passes through the destination point, and the subscript c refers to the location of the center of the spherical FZ in the CW frame located at the destination point. The FZ coordinate system which we used placed the \hat{x}_{FZ} , \hat{y}_{FZ} , and \hat{z}_{FZ} unit vectors parallel to the CW \hat{x} , \hat{y} , and \hat{z} unit vectors, respectively. The zeros explicitly written in the vector differential terms above result from the fact that the values of x_f , y_f , and z_f equal zero at intercept.

Using these equations as a definitive filter on the success or non-success of any given transfer with $\theta < \theta_{crit}$ - sphere = 57 deg, we have constructed a series of computer programs to evaluate the behavior of the success criteria. It is important to remember that in the case of the spherical FZ, the transfer angle is limited to less than 57 deg.

We first pose the problem of statistical success probability for TDC success, TAC success, and full (TDC + TAC) suc-

cess. In our work we matched 306 possible arrival points with 306 possible departure points uniformly distributed on the spherical FZ. Each of these 93,636 cases were run for four transfer angles, θ . The total sample space consisted of 374,544 uniformly distributed cases, corresponding to a confidence level of 0.99837. Table 2 summarizes the result of this study.

From these data, we make three important conclusions. First, the success probability is low throughout the range of allowable samples; this is true for both the combined TDC + TAC cases, as well as each of the TC's independently. Second, success probability increases strongly with transfer angle (time); although this would be expected, due to the increasing curvature of CW paths with transfer angle (time), this is an important conclusion because it tells eventual LSS operators that rapid transfers around the FZ are impossible, unless the Transfer Vehicle makes a series of short segmental paths over the FZ with a redirecting burn at the end of each segment. The final relevant conclusion from this data set stems from the difference in TDC and TAC success probabilities. Notice that TDC and TAC success probabilities decouple with increasing θ , and that the TAC is generally easier to satisfy. This divergence between TDC success and TAC success implies that different strategies may have to be employed to find transfer paths which satisfy both criteria; this result will figure more prominently as we examine more data.

The next result we obtained by examining the value of θ at which each success occurred. In this context, we were only interested in complete success; that is, cases in which both TDC and TAC were satisfied. Figure 4 presents a normalized graph of integrated (i.e., total) number of successes which occurred in our data set by each given value of θ . From these data, we conclude that 1) there is a minimum (lower bound) on ϕ (ϕ_{\min}) which permits success, 2) the number of successes generally increases with θ , and 3) the integrated number of successful cases is as smooth, nearly linear monotonic function of θ . We also find that the lower limit θ_{\min} is generally proportional to the angular separation between the departure and destination points on the sphere. The existence of a lower bound on θ is important. This is because a lower bound on θ , in combination with the upper bound on the sufficiency of the TC's (when used with the CW equations) effectively traps the existence of a noncolliding solution, as predicted by the tangential conditions. We make the important note that the existence of a noncolliding, single-impulse transfer when $\theta > \theta_{\min} > \theta_{\text{crit}}$ is not ruled out by our results; instead, we conclude that the tangential conditions alone cannot predict success when θ exceeds θ_{crit} , and that one cannot, therefore, rely upon the computational simplifications introduced by the sufficiency of the TC's above θ_{crit} .

We next made a study of the behavior of each successful transfer to determine if the value of θ at which success first occurred acted to guarantee success at θ greater than the "opening" θ where success first occurred. We found that in all but two of the 14,607 successful cases (i.e., 0.9987%), success occurred for every value of θ greater than the opening value (θ_{\min}) up to the 57-deg limit on the validity of the TC's as a sufficient condition. Because we used a sphere for our FZ geometry in this test case, we did not conduct tests for θ larger than 57 deg. The important implication here is that once the value θ_{\min} is found (i.e., the shortest value of θ for which a successful transfer could be accomplished), any larger value of θ

would almost certainly be successful, at least to a confidence of nearly 3σ and up to the 57-deg limit on the validity of the TC's as a sufficiency condition. Success, it seems, is effectively continuous between θ_{\min} and 57 deg, wherever θ_{\min} may occur. Investigators interested in future path-constrained rendezvous research will find such a result useful, since it again greatly reduces the numerical workload. More importantly, this result implies that optimization of path-constrained transfer (at least for spheres) can proceed without regard to the path constrained so long as the optimization retains $\theta_{\min} < \theta < 57$ deg as a constraint on the independent variable $\tau = \theta/\omega$.

As a final contribution to this study, we constructed a computer simulation program which produced maps of the region on the unit sphere from which any specified point on the sphere could be reached. Figures 5a-c depict examples of the output of this program. By studying 324 frames such as these (81 fixed departure points with θ set to 15, 30, 45, and 57 deg for each), we were able to draw a number of conclusions. In our tests, the grid on the arrival location was one deg in "sphere latitude" and one deg in "sphere longitude." The most important conclusion reached by this graphic representation of our data was that the region of accessibility (i.e., those points which could be reached from any given departure point) was, regardless of θ , a simply connected, continuous patch on the sphere. In every case, the destination point itself was contained in the accessibility region.

We also found that the area of this patch grew in proportion with the transfer angle; this confirms and explains the earlier result that success probability is proportional to θ . The growth in the area of the accessibility region was generally found to be due to latitudinal broadening, as opposed to circumferential (longitudinal) broadening. By examining the accessibility region itself, it was learned that a) the patch was always symmetrical in latitudinal height above and below the target point, b) travel was limited to less than about 90 (and never more than 100) deg of longitudinal travel, and c) travel was always found to be preferred in the direction opposite the rotation of the coordinate system. Interestingly, the TAC success region usually led the (geometrically similar) TDC region in terms of arrival longitudes. Because both the TDC and TAC regions formed elliptical patches (except at the poles, where they fanned out due to the decreasing circumference at the poles), their intersection, which defines the accessibility region, tended toward the shape of an ellipse as well. We make note that in no case did we observe our simulation to depict the region of accessibility to include purely latitudinal transfers, which we analytically demonstrated to be impossible for spheres.

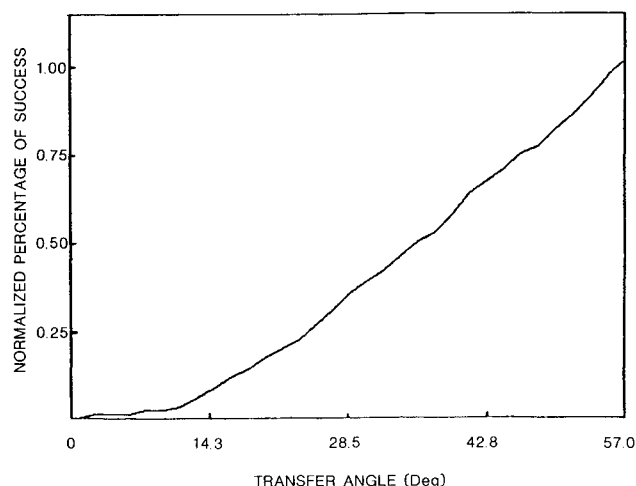


Fig. 4 The integrated number of successes occurring over the interval $[0, \theta]$ to each value up to $\theta_{\text{crit}} = 57$ deg, normalized to a percentage basis, for a spherical FZ. Notice $\theta_{\min} = 3$ deg.

Table 2 A statistical evaluation of transfer success

Success Criteria	Probability of success				
	Average	$\theta = 15$	$\theta = 30$	$\theta = 45$	$\theta = 57$
Fail TDC & TAC	0.939	0.991	0.968	0.928	0.686
Pass TDC only	0.044	0.008	0.026	0.053	0.088
Pass TAC only	0.056	0.008	0.030	0.067	0.119
Pass TDC & TAC	0.039	0.008	0.024	0.049	0.074

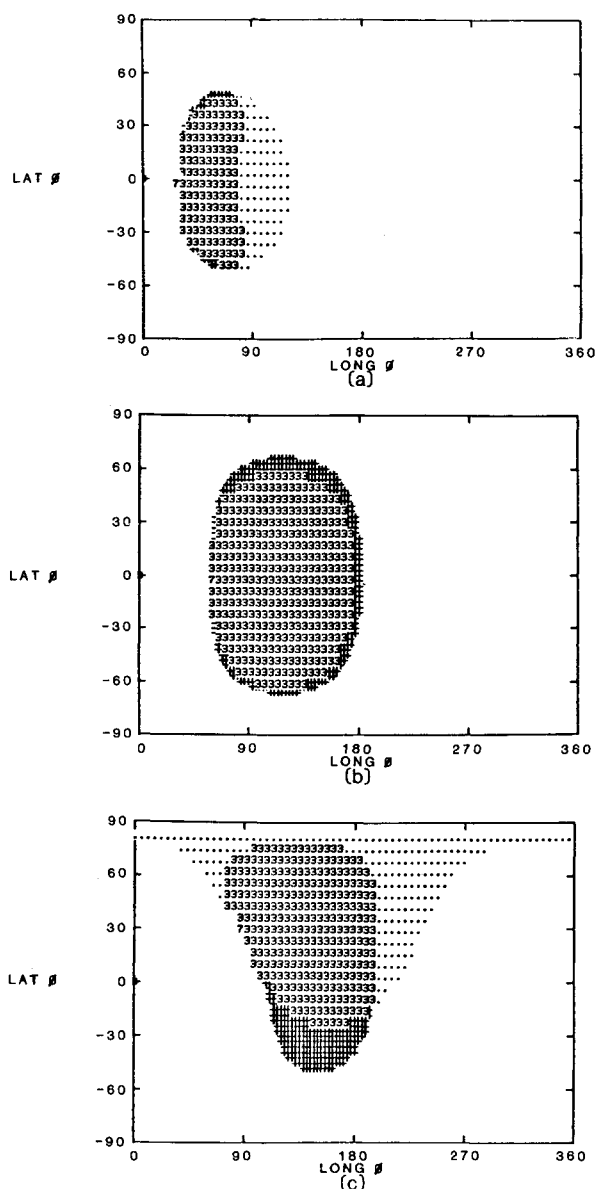


Fig. 5 Maps of the regions from which the point labeled "7" (the destination) can be reached. (+) indicates the TAC is satisfied, (.) indicates the TDC is satisfied, and (3) marks points on this Mercator projection of aspherical FZ where both are satisfied. Notice angular spreading of the TAC-satisfying region near the "north pole" in 5(c).

Architecturally, the connectedness of the accessibility region on a spherical FZ indicates that LSS designers indeed can design the LSS geometry to make possible more efficient operations for vehicles maneuvering in their vicinity during both the construction phase and the operational phase. Operationally, the restricted accessibility region, which was found to always contain the departure point, means that while local single-impulse transfers are possible, global access from any point implies either multiburn "hopping" across the FZ or waypoint strategies, such as those referenced in the Introduction.

VII. Conclusions

We have extended earlier results concerning path-constrained rendezvous in the vicinity of large Space Structures. We first found that LSS size and orbital period could be removed from the formulation by means of a normalization. We then demonstrated that two necessary analytical conditions exist for the solution of a path-constrained rendezvous about any Large Space Structural or other forbidden zone. We

discovered through numerical simulations that for seven different widely applicable constraint surface geometries relative to the orbital coordinate system, these two necessary conditions are also sufficient, up to an *operationally unrestrictive* transfer time limit, which we call θ_{crit} . These conditions results simplify the operational task involved in locating such a path (or family of paths), and also make possible much larger simulations of this multivariable problem.

By applying these results to a case study of motion in the vicinity of a spherical forbidden zone, and depicting accessible regions on a computer terminal, we found that the places from which a given point is accessible all lie within a single essentially regular patch on the FZ surface which contains the departure point. This patch was also found to behave in a regular way as the target location and rendezvous time were varied. It was learned that travel in the direction opposite the orbital rotation was uniquely 'preferred' by the constraint equations and the relative motion geometry. We also established that transfers between any two given points on a sphere form a monotonic family in θ , the transfer angle, so that once a lower (quickest transfer) bound is established, one is guaranteed (to within our 0.9987 test case confidence level) that every other transfer with $\theta_{min} < \theta < \theta_{crit}$ between these two points will be possible.

Future research in this field should include a study of the accessibility region for other primary FZ's, including plates, straws, and cones, and the optimization of the constraint-avoidance techniques developed by Stern in an earlier report.

One particularly relevant application in the light of recent U.S. research trends would be a study of orbital mine-field avoidance. In such a formulation, the mine field would consist of a finite collection of disjoint forbidden zones (each itself of connected geometry), moving in relation to one another according to the theory of satellite cluster relative motion.

Acknowledgments

The first author thanks Dr. Michael Spivak of Rice University for a useful discussion. The second author thanks Dr. George Lawrence of the University of Colorado for a useful discussion about the meaning of the FZ accessibility region. Both authors mention the support of Ms. MDS, Ms. CJS, Ms. BDS, and Ms. LAP in the preparation of our report.

References

1. Stern, S.A., "Extra-Vehicular Point to Point Transfers in the Vicinity of Large Space Structures," Thesis, University of Texas at Austin, 1980.
2. Stern, S.A., "Rectilinear Guidance Strategy for Short Orbital Transfers," *Journal of Spacecraft and Rockets*, Vol. 21, Nov.-Dec. 1984, pp. 542-545.
3. Stern, S.A. and Fowler, W.T., "Path Constrained Rendezvous Near Large Space Structures," *Journal of Spacecraft and Rockets*, Vol. 22, Sept.-Oct. 1985, pp. 548-553.
4. Clohessy, W.H., and Wilshire R.S., "A Terminal Guidance System for Satellite Rendezvous," *Aero/Space Science*, Vol. 27, 1960, p. 563.
5. Dunning, Robert, S., "The Orbit Mechanics of Flight Mechanics," NASA SP-325, 1975, pp. 1-57, 79-84.
6. Farris, R.L., "One and Two Impulse Rendezvous Trajectories," Master's Thesis, University of Texas at Austin, 1979.
7. Lutze, F.H., "Unaided EVA Intercept and Rendezvous Charts," *Journal of Spacecraft and Rockets*, Vol. 16, Nov.-Dec. 1979, pp. 426-431.
8. Mueller, D.D., "Relative Motion in the Docking Phase of Orbital Rendezvous," AMRL-TDR-62-124, 6570 Aerospace Medical Research Labs., Aerospace Medical Div., Wright-Patterson AFB, OH, Nov. 1962.
9. Felleman, F.G., "Analysis of Guidance Techniques for Achieving Orbital Rendezvous," *Advances in the Astronautical Sciences*, Vol. 11, 1964, p. 191.
10. London, H.S., "Second Approximation to the Solution of the Rendezvous Equation," *AIAA Journal*, Vol. 1, July 1963, pp. 1690-1693.